Utah State University

DigitalCommons@USU

Space Dynamics Lab Publications

Space Dynamics Lab

1-10-2013

Far-Infrared Spectroscopy of the Troposphere: Instrument Description and Calibration Performance

Harri Latvakoski
Utah State University

Martin G. Mlynczak
Utah State University

David G. Johnson
Utah State University

Richard P. Cageao
Utah State University

David P. Kratz
Utah State University

Richard P. Cageao
Utah State University

Follow this and additional works at: https://digitalcommons.usu.edu/sdl_pubs

See next page for additional authors

Recommended Citation

Authors

Harri Latvakoski, Martin G. Mlynczak, David G. Johnson, Richard P. Cageao, David P. Kratz, Richard P. Cageao, David P. Kratz, and Kendall Johnson

Far-infrared spectroscopy of the troposphere: instrument description and calibration performance

Harri Latvakoski,[1] Martin G. Mlynczak,[2,*] David G. Johnson,[3] Richard P. Cageao,[3] David P. Kratz,[2] and Kendall Johnson[1]

[1]Space Dynamics Laboratory, 1695 North Research Park Way, North Logan, Utah 84341, USA

[2]Science Directorate, NASA Langley Research Center, Mail Stop 420, Hampton, Virginia 23681, USA

[3]Engineering Directorate, NASA Langley Research Center, Mail Stop 468, Hampton, Virginia 23681, USA

*Corresponding author: m.g.mlynczak@nasa.gov

The far-infrared spectroscopy of the troposphere (FIRST) instrument is a Fourier transform spectrometer developed to measure the Earth's thermal emission spectrum with a particular emphasis on far-infrared (far-IR) wavelengths greater than 15 μm. FIRST was developed under NASA's Instrument Incubator Program to demonstrate technology for providing measurements from 10 to 100 μm (1000 to 100 cm^{-1}) on a single focal plane with a spectral resolution finer than 1 cm^{-1}. Presently no spectrometers in orbit are capable of directly observing the Earth's far-IR spectrum. This fact, coupled with the fundamental importance of the far-IR to Earth's climate system, provided the impetus for the development of FIRST. In this paper the FIRST instrument is described and results of a detailed absolute laboratory calibration are presented. Specific channels in FIRST are shown to be accurate in the far-IR to better than 0.3 K at 270 K scene temperature, 0.5 K at 247 K, and 1 K at 225 K.   © 2013 Optical Society of America

OCIS codes: 010.0010, 010.0280, 010.7030.

1. Introduction

Over the last 20 years the importance of direct far-infrared (far-IR) measurements of Earth's emission spectrum has become widely recognized. The far-IR contains approximately one-half of the Earth's outgoing longwave radiation and greenhouse effect [1], it is responsible for almost all the radiative cooling of the free troposphere [2], and cirrus clouds exert a strong radiative effect in the far-IR [3]. Harries *et al.* [4] summarize the importance of the far-IR to the Earth's climate system.

The far-infrared spectroscopy of the troposphere (FIRST) instrument was developed under NASA's Instrument Incubator Program to demonstrate technology (in a space-like environment) for measuring the far-IR spectrum (15–100 μm; 650–100 cm^{-1}). To enable comparisons with extant IR spectrometers, the required spectral range of FIRST was set to be 10–100 μm (1000–100 cm^{-1}). FIRST was built by the Space Dynamics Laboratory (SDL) in Logan, Utah, in collaboration with the NASA Langley Research Center. In June 2005 the FIRST instrument successfully conducted an engineering demonstration flight on a high altitude balloon over Fort Sumner, New Mexico [5]. A second balloon flight was conducted in September 2006. Subsequent to that the instrument scene selection assembly was modified to enable FIRST to operate as a ground-based spectrometer observing downwelling radiation from the atmosphere by viewing in the zenith direction.

The FIRST spectrometer has since participated (with several other instruments) in a major atmospheric field campaign in the Atacama Desert in Chile in late 2009. During this campaign the first measurement of the entire Earth's IR emission spectrum was made [6].

In 2011 the FIRST instrument was returned to SDL for absolute radiance recalibration in anticipation of future atmospheric observation campaigns. The results of this recalibration are described in this paper and are essential for interpreting far-IR spectra measured by the FIRST instrument. The instrument is described in Section 2. The calibration equipment and testing are described in Section 3. The calibration results are described in Section 4. Section 5 is the conclusion.

2. FIRST Instrument Description

The FIRST instrument is a Fourier transform interferometer with a germanium-on-polypropylene thin film beam splitter to provide a spectral resolution of 0.643 cm^{-1} and a spectral response over the required 100–1000 cm^{-1} spectral range [7]. As will be shown below, FIRST response is from 4.54 to 200 μm, 2200 to 50 cm^{-1}.

The interferometer is a porch swing design recording double-sided interferograms with a mirror travel (including turn around) of ∼0.5 cm either side of center (i.e., zero optical path difference). A helium–neon (He–Ne) metrology laser is used to determine the sampling location. FIRST samples every fringe of the He–Ne laser, and 24,576 points are collected for each interferogram, which results in 1.55 cm of total optical path difference change and 0.78 cm in total physical travel and gives a resolution of 0.643 cm^{-1}. Data collection time for one scan is 11.5 s including turnaround time.

The FIRST aperture is quite large at 7 cm and is due to an original requirement set early in the FIRST program to demonstrate instrument technology that could record the entire IR spectrum over nearly the entire Earth at less than 20 km pixel size on a daily basis from low Earth orbit. This requirement resulted in the need for a 100-element focal plane (sized at 10×10 elements) to achieve the required measurement of over 5 million spectra per day.

The FIRST detectors are silicon bolometers, each with a 0.41° field of view. To minimize cost, the FIRST instrument focal plane is populated with 10 (not 100) detectors, two at each corner of the focal plane and two in the center. This layout was decided upon to verify that the optical throughput of the instrument was sufficient to completely fill the entire focal plane area and to provide redundant detector capability. The focal plane has a total field of view of $4.4° \times 4.4°$ and corresponds to a total throughput of 0.42 cm^2 sr. The FIRST detectors are behind Winston cones and are cooled to 4.2 K with liquid helium in order to meet the single spectrum precision goals of the instrument. Two on-board blackbodies are used for instrument calibration, an ambient

blackbody (ABB) and a warm blackbody (WBB) that is heated to ∼30 K above ambient. For balloon flights the WBB is removed to provide a view of space to more readily simulate the calibration approach on an orbiting satellite. Table 1 lists the basic FIRST instrument parameters and performance goals. The radiometric precision goals of FIRST are expressed as NEΔT for a single spectrum of a target at 230 K. The absolute accuracy goal of the instrument was established to be identical to the precision, acknowledging the intent to average many spectra to substantially reduce random noise in the overall error budget. It will be demonstrated in Section 4 that FIRST does meet these goals for a range of target (scene) temperatures.

The FIRST Instrument (Fig. 1) is housed inside a vacuum container to simulate the environment of space and to enable the instrument to operate at different temperatures. The sturdy housing also enables the instrument to survive landings by parachute at the end of high altitude balloon flights. FIRST consists of three sections separated by vacuum windows: the scene select assembly, the interferometer section, and the detector dewar. The vacuum windows are made of 41 μm thick polypropylene. The window between the detector dewar and interferometer section is a single sheet of polypropylene, while the window between the interferometer section and the scene select assembly is made of two sheets in series for increased strength. The window between the interferometer and the scene select assembly is required because the scene select assembly is exposed to air during atmospheric observations, while the window between the detector dewar and the interferometer section, which is not strong enough to hold one atmosphere of pressure, limits condensation onto the cold detectors.

The detector dewar contains the focal plane assembly and cryogen tanks. The interferometer section contains the interferometer and the aft optics that focus the beam from the interferometer onto the detectors. There are no imaging fore optics. The interferometer section can be cooled with liquid nitrogen (LN_2) to 180 K to demonstrate that the interferometer can operate over a range of temperatures. For ground observations and for the calibration described here, this section is kept under vacuum, but at ambient temperature. The scene select assembly contains a rotating mirror that directs the incoming

Table 1. FIRST Instrument Parameters and Performance Goals

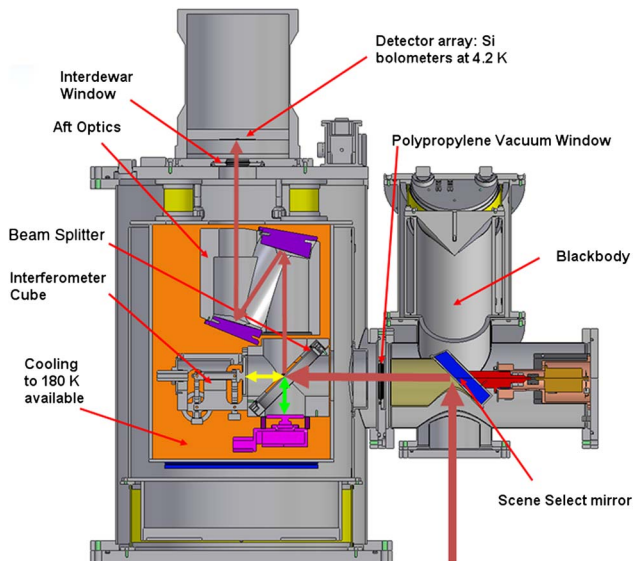|	
Spectral range	100–1000 cm^{-1} (with some coverage 50–2200 cm^{-1})
Resolution	0.643 cm^{-1}
Scan time	11.5 s
Aperture	7 cm
Focal ratio	$f/6.5$
Field of view	10 0.41° FOV detectors in a sparsely populated $4.4° \times 4.4°$ FOV
NEΔT	0.2 K, 170–1000 cm^{-1}; 0.5 K 100–170 cm^{-1}; at 230 K (performance goal)

Fig. 1. (Color online) Cutaway view of FIRST with the principal components labeled and the light path shown by the thick red arrows.

Fig. 2. (Color online) Cutaway view of the LWIRCS blackbody.

beam to one of three ports: the instrument aperture or one of two calibration ports. The entire scene select assembly can be rotated where it attaches to the interferometer section so that an open port can face up (for making atmospheric observations from the ground) or down (for observations from a balloon) or to the side (for calibration in the laboratory). The scene select assembly is normally positioned to observe the outside during atmospheric data collection. Calibration scenes are typically observed at the beginning and end of each atmospheric observation sequence. Except for the detector amplifiers, the electronics that control and read out FIRST are in a separate container and are entirely commercial off-the-shelf boards and computers.

3. FIRST Ground Calibration

FIRST was calibrated for absolute radiance by attaching the long wave infrared calibration source (LWIRCS) blackbody to the third port of the scene select assembly. LWIRCS [8] (Table 2, Fig. 2) is a ground calibration blackbody of a similar design to the FIRST on-board blackbodies. This design [9] uses specular Z302 paint and a specular trap design to achieve high emissivity. The shape of the LWIRCS cavity ensures that any ray exiting the blackbody at near-normal incidence can be traced backward through at least five specular reflections before the
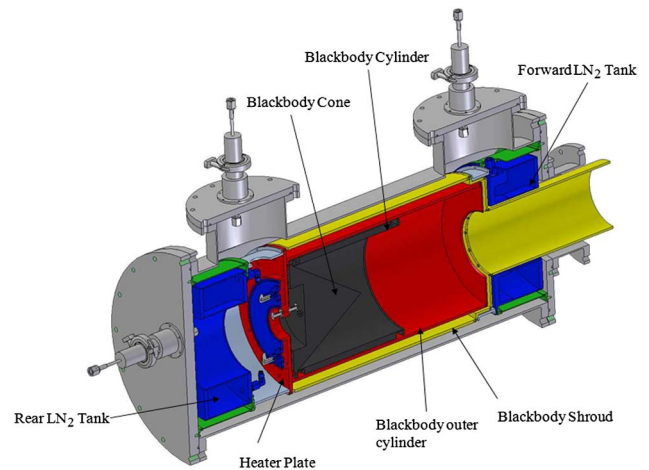
Table 2. Performance Specifications for the LWIRCS Blackbody

Wavelength range	1–100 μm
Temperature range	90–350 K
Aperture	6.1 in. (15.5 cm)
Beam divergence accepted	6° full angle
Emissivity	≥0.9998 (1–35 μm); ≥0.9980 (35–100 μm)
Temperature uncertainty	~130 mK

path leaves the blackbody. This reduces blackbody reflectivity caused by the specular reflectance of Z302 to negligible levels. Blackbody reflectivity caused by the small diffuse component of Z302 reflectance is minimized by the distance between the back of the cavity and the blackbody aperture. The LWIRCS cavity consists of a cone that points toward the aperture surrounded by three concentric cylinders. The thick, conductive cone minimizes thermal gradients across its surface, and the concentric cylinders minimize thermal gradients by minimizing radiative heat loads on the inner cavity from the surroundings. Heaters for the cone and inner cavity are located on a heater plate behind the cone to minimize effects of uneven heating. LWIRCS has two separate LN_2 tanks to provide the proper amount of cooling over its large temperature range. One tank is conductively coupled to the heater plate and provides cooling for temperatures below 230 K. For higher temperatures this tank is unfilled and the radiative coupling from a second LN_2 tank provides the cooling.

The output of LWIRCS has been measured with the National Institute of Standards of Technology (NIST) transfer radiometer (TXR) [10]. The TXR is a radiometer with two bands, one centered at 5 μm and one centered at 10 μm. Each band is approximately 1 μm wide, with a brightness temperature scale based on a NIST water bath blackbody. The TXR measurement uncertainty is approximately 90 mK at 5 μm and about 150 mK at 10 μm.

When observed with the TXR, the LWIRCS brightness temperature agrees with the LWIRCS temperature to within 95 mK (maximum deviation) at 5 μm from 210 to 350 K, and to within 186 mK at 10 μm from 180 to 350 K [11]. The agreement is at approximately the TXR measurement uncertainty level. During this test, the emissivity of LWIRCS was measured with the TXR and a heated halo-type test to be 0.99969 ± 0.00003 at 5 μm. This result is consistent with the calculated value of 0.9998, because the method used to perform the test reduces the LWIRCS emissivity from the calculated case.

The FIRST instrument is calibrated with LWIRCS by setting LWIRCS to a specific temperature and conducting a data collection sequence in which the ABB is observed for 4 min, LWIRCS for 7 min, and then the WBB for 4 min. This sequence is repeated once for each LWIRCS temperature in the range from 170 to 330 K in steps of ~20 K. LWIRCS required several hours to change temperature and become stable at the new temperature. Calibration data were collected in October 2011 and in February 2012. In all cases the ABB was held at a temperature near 293 K, and the WBB was held at 324 K.

A. FIRST Calibration Data Processing

A general fast Fourier transform algorithm and associated processing is used to process the FIRST interferograms into spectra. In addition, there are three further steps that are taken to achieve the final calibrated FIRST spectra: gain combination, exclusion of bad data, and phase alignment. These processes are described in this section.

Achieving the sensitivity levels for FIRST requires a 20 bit dynamic range in the interferogram. At the time FIRST was developed, commercial 20 bit analog-to-digital converters that would meet the needs of FIRST were not available. Instead, FIRST is designed to collect two sets of data per detector, with the second simultaneous set collected at a 100 times higher gain setting than the first. The two gain channels are combined by using high gain data when it is sufficiently below the previously derived saturation level. Interferogram signal levels are such that low gain data are used only near the centerburst. When combining data, the high gain data are multiplied by a factor and an offset is added, with the factor and offset determined from comparing high and low gain output in calibration data. The low gain data account for approximately half of the noise in a spectrum.

FIRST uses a thin film beam splitter in the interferometer that is susceptible to vibration. Such vibration will affect the spectra and was observed early on in the development of FIRST. The effects were mitigated by sampling at every fringe of the He–Ne laser. This puts the Nyquist wavenumber at 7899 cm⁻¹ and transfers the major effects of vibration to a region of the spectrum (2500–3200 cm⁻¹) with no atmospheric signal of interest. With this change, the effects of vibration are reduced to acceptable levels for most spectra. Occasionally, outside sources add excessive vibration to some interferograms that must be excluded as bad data. High vibration is visible in the transformed interferogram as a broad peak from 2250 to 3000 cm⁻¹, as shown in Fig. 3.

The last step in the data processing prior to absolute calibration is correcting the interferograms for phase alignment. The FIRST beam splitter is not transparent at the He–Ne laser wavelength due to the Ge coating, and it was not possible to leave a small clear section on the beam splitter to transmit the He–Ne laser. For FIRST the He–Ne metrology laser has its own separate beam splitter and
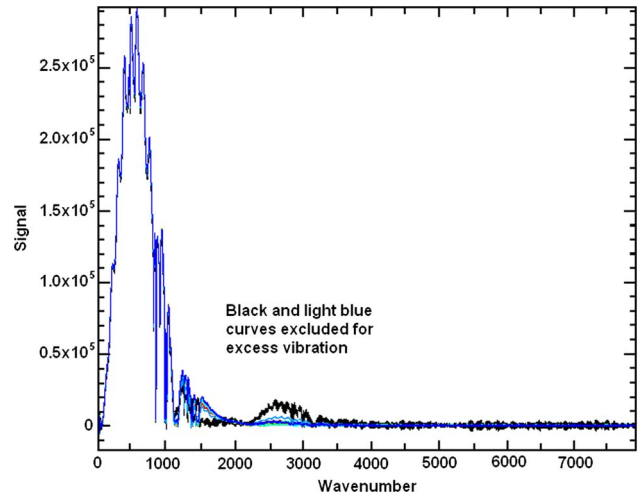

Fig. 3. (Color online) Ten full-resolution FIRST spectra from detector 3. Excess vibration is present in some spectra and evident as a broad peak around 2700 cm⁻¹.

illuminates a polished section on the backside of the moving mirror. This effectively provides position information for the moving mirror. However, thermal expansion can differentially change the optical path of the laser and the input IR beam from the atmosphere or calibration sources. This results in a shift of the sampling positions with respect to the peak of the interferogram, which in turn results in the shift of the phase in the spectrum produced from the interferogram.

FIRST also has out-of-phase light present in the spectra, and thus the interferogram phase will differ for targets with different radiance levels. Figure 4 shows both the variation in phase with target and
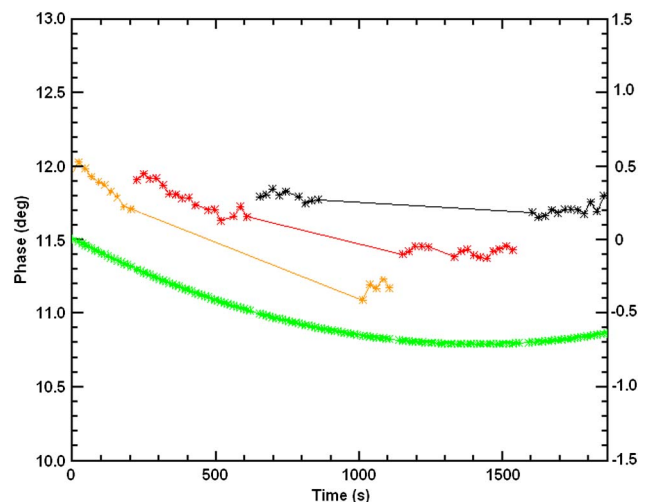

Fig. 4. (Color online) Phase (left axis) for all good scans in the forward direction for detector 3 at 514 cm⁻¹ with 15.4 cm⁻¹ resolution for the data set where LWIRCS was at ~310 K. Orange (third from top) is the ABB data, red (second from top) is LWIRCS data, and black (top) is the WBB data. The green (bottom) curve (right axis) is the phase correction function at 514 cm⁻¹, which shows the amount subtracted from all forward direction phases to correct for the drift.

the drift in phase at 514 cm^{-1} averaged over ~15 cm^{-1} from a data set with LWIRCS at ~310 K. The drift in phase produced by differential change in the optical path is a simple linear function of the wavenumber, so it is sufficient to measure the phase over a limited spectral range. The drift in phase is corrected, while maintaining the difference in phase between targets, by fitting a line to the WBB and ABB data and combining these to give a quadratic phase correction curve (see Fig. 4). To align the phase in all scans, spectra are shifted in phase by the amount of the correction curve at 514 cm^{-1} with proportional scaling at other wavenumbers. In practice, this aligns the phases to ~0.2°, below which phase errors are not significant.

B. Calibration Spectra

For each detector, the resulting good spectra (i.e., those not excluded for high vibration or other problems) were averaged for each target with separate averages kept for each direction of the mirror movement. The six (forward and backward spectra for the ABB, WBB, and LWIRCS) resulting average spectra per detector for each data set are complex numbers. These spectra were used to examine detector nonlinearity and to calculate responsivity and the LWIRCS radiance and brightness temperature. Figure 5 shows three averaged spectra of the WBB in the forward direction from detector 3. The changes in the spectra are changes over time in the FIRST response and changes in phase.

C. Nonlinearity

Detector nonlinearity will produce artifacts in the spectrum realized from a transformed interferogram. The most consistent and obvious artifact, regardless of the functional form of the nonlinearity, will be a broad hump of increased signal near zero
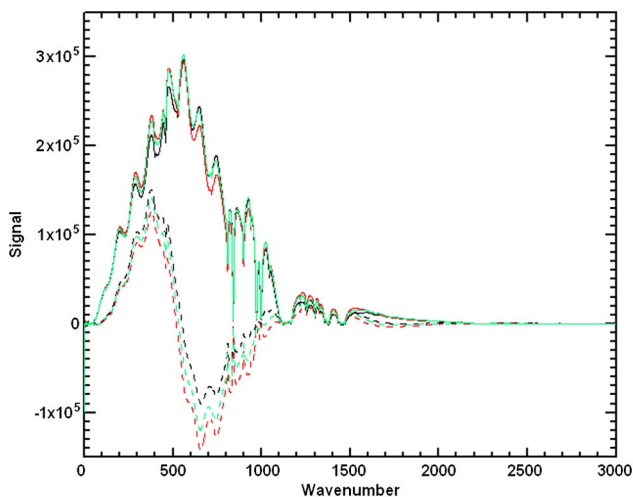

Fig. 5. (Color online) Three average spectra of the WBB in the forward direction from detector 3 at full 0.6428 cm^{-1} resolution. The real part is the solid curve and the imaginary part is the dashed curve.
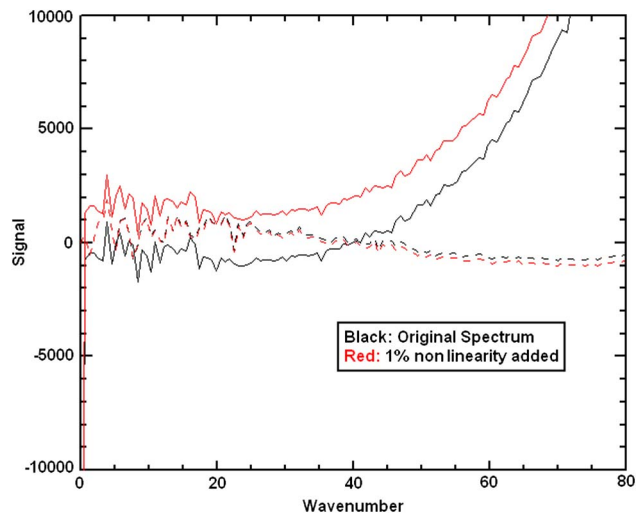

Fig. 6. (Color online) Low wavenumber section of an averaged forward direction spectrum of the WBB from detector 3 and the same spectrum with 1% nonlinearity added to the interferograms. The solid curves are the real parts and the dashed curves are the imaginary parts.

wavenumber. Figure 6 shows the low wavenumber end of an averaged $\overline{\text{WBB}}$ spectrum from detector 3, with little noise at the low wavenumber end, and the same spectrum with nonlinearity added to the interferogram using

$$I \to I + aI^2, \qquad (1)$$

where I is the interferogram and a is a constant chosen to increase the signal at the peak of the interferogram by 1%. This is a quadratic nonlinearity, which for a small amount of nonlinearity is nearly always the first term to appear. Higher order nonlinearity terms have a similar effect at low wavenumbers as the quadratic.

Without the added nonlinearity, both the real and imaginary parts of the FIRST spectra tend toward zero at zero wavenumber. With the nonlinearity added, the imaginary part is relatively unchanged while the real part rises noticeably above zero. The obvious change from a small added nonlinearity shows the FIRST data is consistent with detector 3 being linear to better than ~0.3%. Similar results are found for all detectors and for spectra of the ABB and LWIRCS as well. This shows the FIRST detectors to be quite linear. In general, the effect of nonlinearity on a spectrum at wavenumbers where a signal is present is comparable in magnitude to the fractional nonlinearity in the interferogram; therefore, nonlinearity in the FIRST spectra cannot be much above this level. Nonlinearity would also be apparent in the FIRST calibration spectra of LWIRCS at various temperatures as a deviation in the observed versus expected LWIRCS spectra that varies systematically with LWIRCS temperature. Such a variation is not observed above the level of other noise sources (see Section 4), so nonlinearity is not

a significant contributor to FIRST uncertainty and no correction for nonlinearity is made.

D. Responsivity

The FIRST responsivity (observed signal divided by the radiance entering the aperture) is calculated using the following expression:

$$\Re = \frac{S_{\mathrm{WBB}} - S_{\mathrm{ABB}}}{P(T_{\mathrm{WBB}}) - P(T_{\mathrm{ABB}})}. \qquad (2)$$

Here $\Re$ is the responsivity, S is the complex spectra observed from the WBB and ABB, P is the Planck function, and T is the temperature of the WBB and the ABB. The responsivity is a function of wavenumber, is calculated separately for each direction of mirror movement, and is a complex number. The responses for forward and reverse directions are nearly, but not exactly, complex conjugates. The response is calculated separately for each LWIRCS data set and is observed to change over time. The blackbody emissivity is taken to be 1.0, since for the ABB the emissivity is effectively 1.0, as the surroundings are at the same temperature. The WBB has an expected emissivity of greater than 0.9985, which is sufficiently close to 1.0 to have a minimal effect on the FIRST calibration.

Figure 7 shows the measured FIRST response. The oscillations from 100 to 800 cm^{-1} are features of the polypropylene windows, as are the sharp drops near 825 and 1000 cm^{-1} and the broad reduction in response above 800 cm^{-1}. The broader no-response regions at 1100 and 2200 cm^{-1} are regions of low beam splitter efficiency. Above 2200 cm^{-1} there is little response and the effects of vibrations dominate. The shape of the response curve is similar for all detectors, with some variation in magnitude.

E. LWIRCS Radiance

The FIRST calibration equation is given by

$$R_{\mathrm{Target}} = \frac{S_{\mathrm{Target}} - S_{\mathrm{ABB}}}{\Re} + P(T_{\mathrm{ABB}}). \qquad (3)$$

S_{Target} is the signal measured by FIRST viewing the target under observation, R_{Target} is the target radiance, and $\Re$ is the responsivity calculated from Eq. (2). Figure 8 shows the LWIRCS radiance measured by FIRST and using Eq. (3) with LWIRCS at several temperatures.

4. FIRST Absolute Calibration Results

The LWIRCS brightness temperature is calculated from the FIRST LWIRCS radiances using the inverse Planck function. No correction is made for the blackbody emissivity being less than 1.0, because the difference is not significant when assessing the overall uncertainty of the FIRST instrument. The brightness temperatures measured by FIRST when observing LWIRCS are compared with temperatures from the LWIRCS temperature sensors to assess the absolute calibration of FIRST.

Figure 9 shows the brightness temperature measured when LWIRCS is at 292.76 K (room temperature, with LWIRCS unheated and without cryogen). The ABB was at 293.66 K during this measurement. Between 200 and 1000 cm^{-1}, excluding the narrow regions of low response, the brightness temperature agrees with the LWIRCS temperature to within 0.2 K. The rms deviation from 200 to 800 cm^{-1} is 0.067 K.

The random noise component in the brightness temperature is the rapid variation from spectral bin to spectral bin, which increases at high wavenumbers, low wavenumbers, and any other regions where
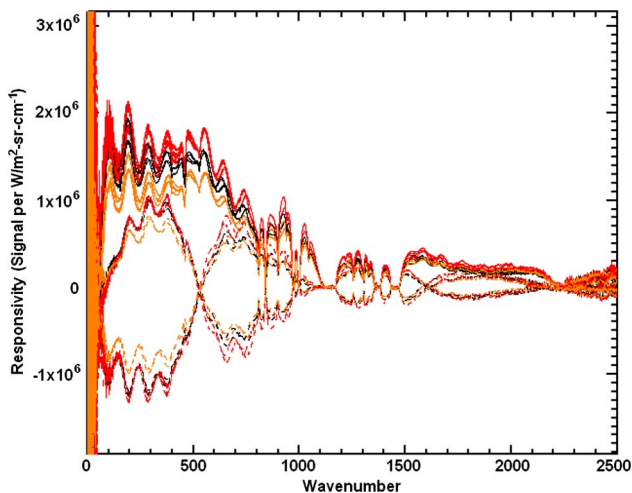

Fig. 7. (Color online) FIRST response for detectors 1, 2, and 3 (black, red, and orange, respectively) and both directions for two calibration data sets. The other detector responses are within the range shown by these three.
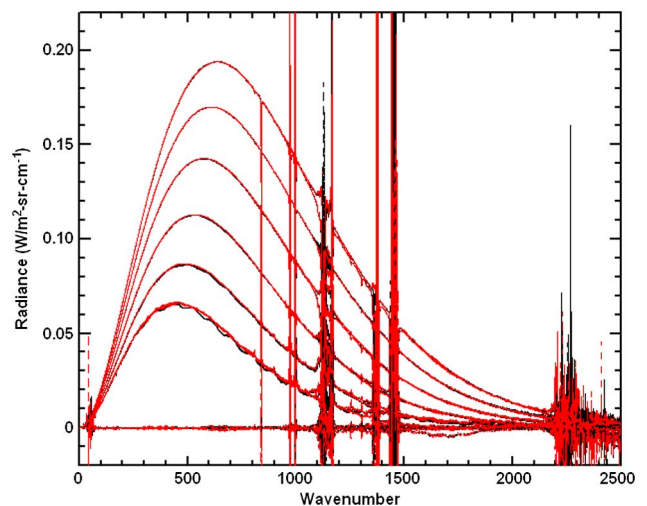

Fig. 8. (Color online) LWIRCS radiance from detectors 1 and 2 for LWIRCS at 324, 310, 293, 271, 247, and 225 K. The measured radiances from the other detectors fall on top of these curves. The traces along and near the zero radiance lines are the imaginary parts of the radiance spectrum.
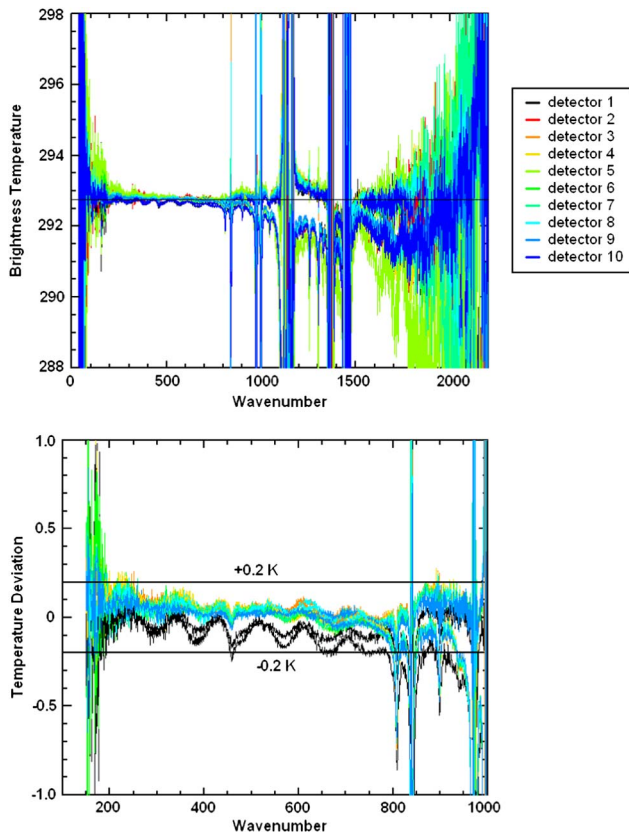
Fig. 9. (Color online) Top: Brightness temperature for LWIRCS at 292.76 K as measured by each detector from 50 to 2200 cm^{-1}. Both scan directions are shown in the same color. The horizontal black line is 293.76 K. The resolution is 0.6428 cm^{-1}. Bottom: brightness temperature deviation over the 150–1000 cm^{-1} range for all detectors except 2, 5, and 10. The rms deviation (average for all detectors here) from 200 to 800 cm^{-1} is 0.067 K.

FIRST response is low. At the low wavenumber end, this noise also is increased, because the difference in spectral radiance between WBB and ABB is reduced (it is 13% at 100 cm^{-1}, compared to 30% at 500 cm^{-1}). The brightness temperatures for the two mirror travel directions trace each other closely below 900 cm^{-1} but diverge at higher wavenumbers, with all detectors showing the same divergence. This noise component is most likely vibration, because it changes from scan to scan but affects all detectors the same way. Data from detectors 2, 5, and 10 are excluded from the temperature deviation plots in Fig. 10 and all subsequent deviation plots, because detectors 2 and 10 show intermittent noise, which degrades their performance at some LWIRCS temperatures, and detectors 5 and 10 show sensitivity to stray light, which degrades their performance.

By Eq. (3), the Fig. 9 data set is essentially a comparison of the ABB with LWIRCS. Since both are at ambient temperature, blackbody reflectivity will minimally affect the measurements, so this data is entirely a comparison of the ABB and LWIRCS temperatures. The temperatures agree to within 0.1 K, which is approximately the estimated uncertainty in the temperature sensors.
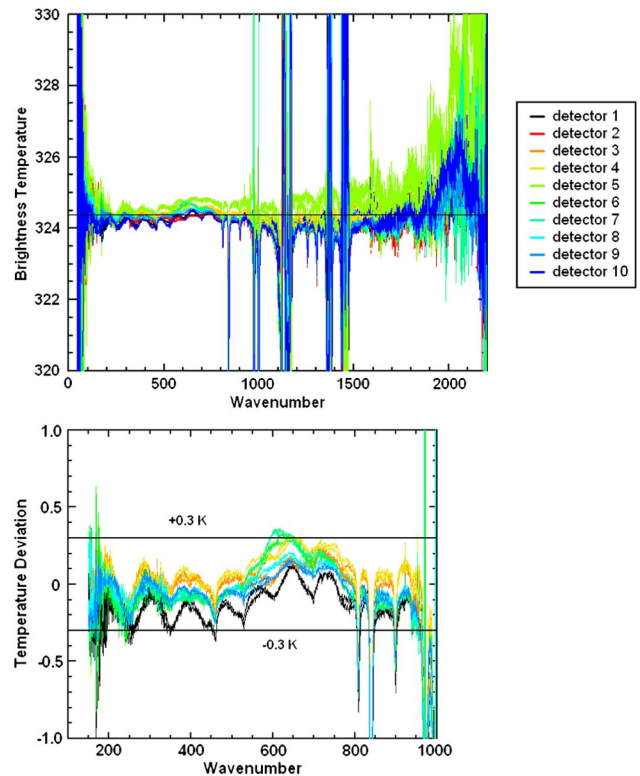

Fig. 10. (Color online) Top: brightness temperature for LWIRCS at 324.38 K for all detectors. Both scan directions are shown in the same color. The horizontal black line is 324.38 K. Bottom: brightness temperature deviation over the 150–1000 cm^{-1} range for all detectors except 2, 5, and 10. The rms deviation (average for all detectors here) from 200 to 800 cm^{-1} is 0.13 K.

Figure 10 shows the measured brightness temperature with LWIRCS at 324.38 K. For this data set, the results for both scan directions fall on top of each other, which shows that the noise source present in the previous data set (vibrations) is much reduced here. The oscillations in the brightness temperature visible here are due to some systematic noise component that remains the same for multiple scans. Except for detectors 2, 5, and 10, the brightness temperatures agree with the LWIRCS temperature to within 0.3 K, with the rms between 200 and 800 cm^{-1} 0.13 K.

When the LWIRCS core temperature is at 324.38 K, it is very close to the WBB set temperature of 324.60 K. Therefore, these data are a comparison of LWIRCS with the WBB. To achieve the agreement shown in Fig. 10, the brightness temperature of each blackbody must agree to within 0.1 K, which is again the estimated uncertainty in the temperature sensors. The good agreement between the WBB and ABB with the well-calibrated and NIST-tested LWIRCS and the lack of significant nonlinearity in FIRST indicates that FIRST data can be calibrated using the calibration equation and on-board blackbody temperatures with no additional corrections.

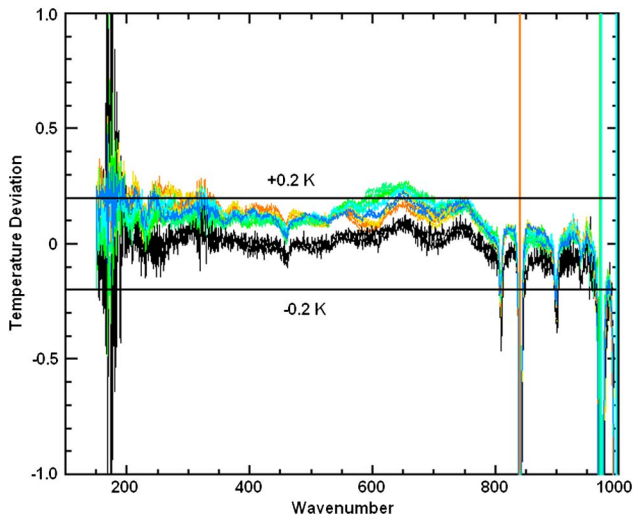Shown in Figs. 11–15 are the deviations of the LWIRCS brightness temperatures measured by

Fig. 11. (Color online) Brightness temperature deviation for LWIRCS at 310.34 K for all detectors except 2, 5, and 10. The rms deviation (average for all detectors here) from 200 to 800 cm^{-1} is 0.13 K.

FIRST from the LWIRCS temperature at temperatures ranging from 169 to 310 K. This range clearly brackets the range of atmospheric scene temperatures. At 310.43 K, the brightness temperature is within 0.2 K of the LWIRCS temperature, and at 270.55 it is within 0.3 K. At colder temperatures, the peak brightness temperature deviations increase, and noise increases especially at the high-wavenumber end. The brightness temperatures are within 1.5 K of the LWIRCS temperature at 209.41 K with the rms deviation remaining below 0.75 K. Deviations are notably higher at lower temperatures. The observed deviations are predominantly systematic over multiple scans, as the results for scan directions generally track each other. The calibration results for 200–800 cm^{-1} are summarized in Table 3.

The increase in brightness temperature noise occurs in part because the dominant noise terms are independent of target temperature, and a given change in radiance is a larger change in brightness temperatures at colder temperatures for wavenumbers above the Planck function peak. This effect is strongest for the higher wavenumbers and limits the accurately calibrated wavenumber range at colder temperatures. The noise also increases at colder temperatures, because errors from spectra of the on-board blackbodies contribute more to the error in calibrated spectra for temperatures outside those of the WBB and ABB. A given amount of error in the ABB radiance causes an error in the measured LWIRCS radiance of

$$\Delta R_{\text{LWIRCS}} = \frac{P(T_{\text{LWIRCS}}) - P(T_{\text{WBB}})}{P(T_{\text{WBB}}) - P(T_{\text{ABB}})} \Delta R_{\text{ABB}}. \quad (4)$$

The ratio of the error in measured LWIRCS radiance to error in the ABB radiance is 1 if LWIRCS is at 293 K of the ABB, but by 169 K this ratio is 4.7 at 200 cm^{-1}, 3.8 at 500 cm^{-1}, and 2.6 at 1000 cm^{-1}. In terms of brightness temperature a 0.1 K error in the ABB propagates to an error in a 169 K LWIRCS of 0.5 K at 200 cm^{-1}, 0.9 K at 500 cm^{-1}, and 3.4 K at 1000 cm^{-1}. This propagation of uncertainty from the ABB occurs for all sources of uncertainty in the ABB spectra, including any systematic effects. Table 4 shows the propagation of 0.2 K ABB temperature uncertainty summed in quadrature with 0.3 K WBB temperature uncertainty to the uncertainty in observed targets at various temperatures. Comparison of the values in this table with the observed LWIRCS deviations suggests some of the increase in deviation at colder temperatures is simply an effect of error propagation.

Figure 15 shows the average difference between brightness temperatures measured by FIRST and the LWIRCS core temperature for all 10 FIRST detectors, averaged over 459.6–559.5 cm^{-1}. The larger differences (that correspond to reduced accuracy) at low temperatures are indicative of systematic errors, but there is no clear trend of deviation versus temperature, as would be expected if this was entirely an effect of error propagation on constant systematic errors. Small changes in systematic error over time,
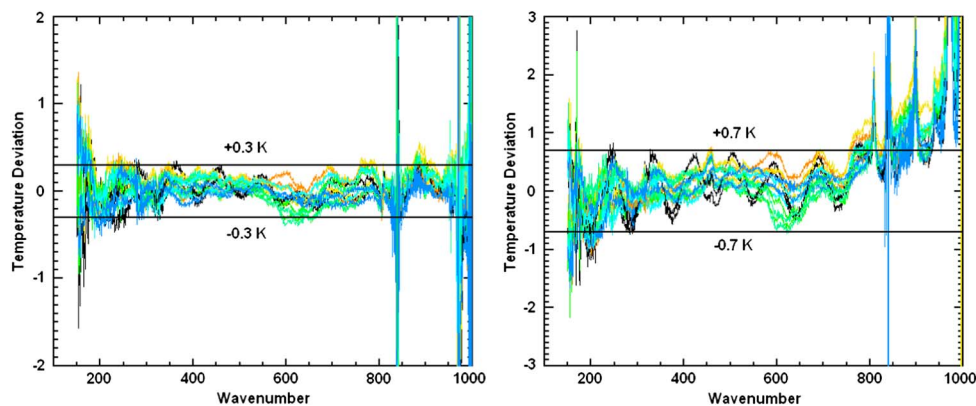

Fig. 12. (Color online) Brightness temperature deviations for LWIRCS at 270.55 K (left) and LWIRCS at 247.42 K (right) for all detectors except 2, 5, and 10. The rms deviations (average for all detectors here) from 200 to 800 cm^{-1} are 0.13 and 0.32 K.
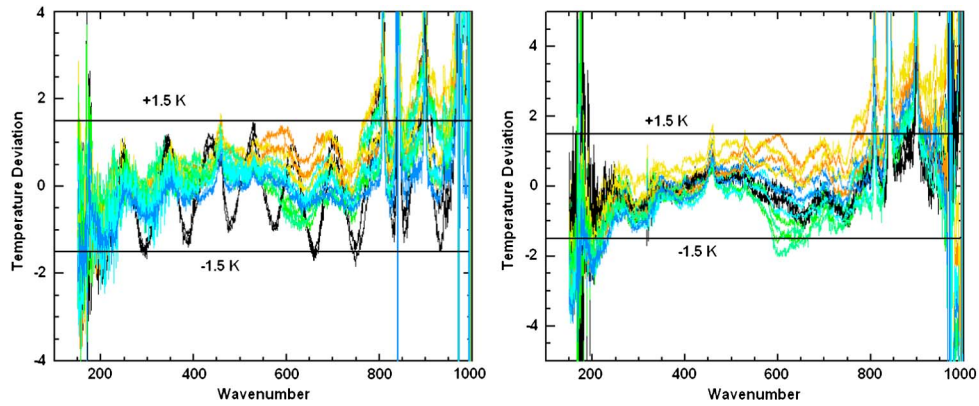
Fig. 13. (Color online) Brightness temperature deviations for LWIRCS at 225.18 K (left) and 209.41 K (right) for all detectors except 2, 5, and 10. The rms deviations (average for all detectors here) from 200 to 800 cm^{-1} are 0.61 and 0.71 K.
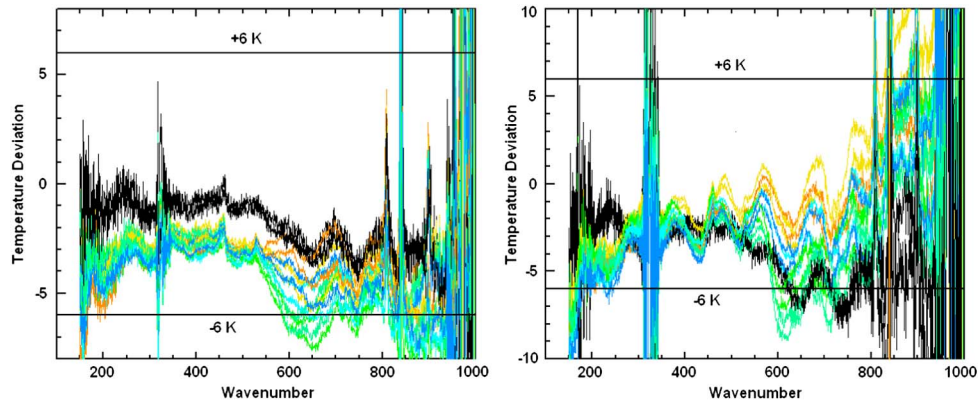

Fig. 14. (Color online) Brightness temperature deviations with LWIRCS at 189.33 K (left) and 169.06 K (right) for all detectors except 2, 5, and 10. The rms deviations (average for all detectors here) from 200 to 800 cm^{-1} are 3.6 and 3.8 K.
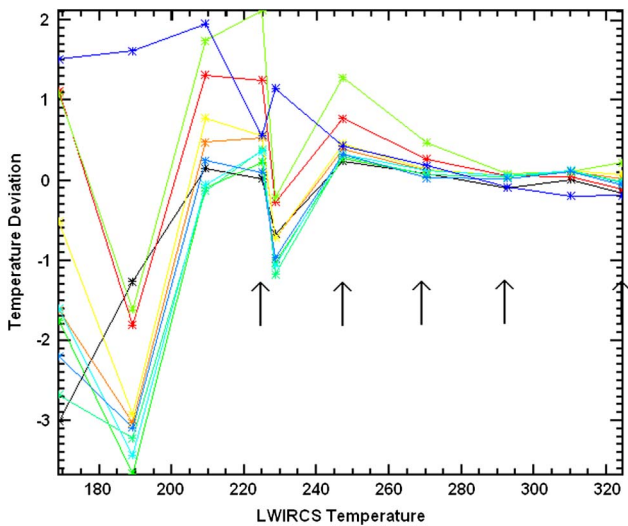

Fig. 15. (Color online) Average brightness temperature deviation from 459.6 to 559.9 cm^{-1} versus LWIRCS temperature for all detectors. Only forward direction data is shown here to reduce clutter, as the reverse data results nearly overlay these. Data were taken at two separate times, with FIRST re-evacuated between collections. The arrows show data taken during the second of the two vacuum cycles.

combined with the error propagation effect, could account for the observed deviations. There is some indication that a vacuum cycle of FIRST will change the deviations, as seen by the change between the LWIRCS temperatures of 225 and 229 K in Fig. 15. The observed ~1 K difference is indicative of the amount of change possible with a vacuum cycle.

A possible source of the observed deviations is stray light. Other calibration data showed that the FIRST detectors are sensitive to light from higher angles than expected, and during this calibration this stray light would consist of room temperature

Table 3. FIRST Absolute Radiometric Calibration and Noise Performance from 200 to 800 cm^{-1}

LWIRCS T (K)	Peak T Deviation (K)	Peak rms T Deviation (K)
310.34	0.2	0.13
270.55	0.3	0.13
247.42	0.7	0.32
225.18	1.5	0.61
209.41	1.5	0.71
189.33	4–7	3.6
169.06	4–9	3.8

Table 4. Propagation of 0.2 K ABB Uncertainty and 0.3 K WBB Uncertainty into Measurements of Targets at Several Target Temperatures and Wavenumbers[a]

Target Temperature	200 cm⁻¹	500 cm⁻¹	800 cm⁻¹	1000 cm⁻¹
225 K	0.9 K	1.1 K	1.4 K	1.7 K
209 K	1.1 K	1.4 K	2.0 K	2.6 K
169 K	1.7 K	2.7 K	5.4 K	8.5 K

[a]The ABB is assumed to be at 293 K and the WBB at 324.5 K.

radiation. Observations of the room temperature ABB would be unaffected by such stray light, but a small change to the observed WBB radiance could again cause significant error at low temperature when combined with the error propagation. The amount of stray light could change with vacuum cycle, since the FIRST windows do not return to the same shape after each pumpdown, and this shape may affect the beam.

5. Conclusions

The recalibration of the FIRST instrument with the NIST-calibrated LWIRCS blackbody shows that for 7 of FIRST's 10 detectors (numbers 1, 3, 4, 6, 7, 8, and 9), the absolute calibration ranges from 0.2 K at warm scene temperatures (∼310 K) to 1.5 K at cold scene temperatures (∼209 K). Between 200 and 800 cm⁻¹ the rms deviation is better than 0.75 K at all scene temperatures greater than 210 K. The result is likely similar for detectors 2, 5, and 10, but stray light and intermittent noise complicated the measurement. At scene temperatures close to the WBB and ABB temperatures FIRST meets the design goal of 0.2 K absolute accuracy from 170 to 1000 cm⁻¹. The observed reduction in accuracy at lower scene temperatures is most likely due to a large increase in propagated error from the on-board blackbodies combined with small systematic errors that change over time.

References

1. M. G. Mlynczak, J. E. Harries, R. Rizzi, P. W. Stackhouse, D. P. Kratz, D. G. Johnson, C. J. Mertens, R. R. Garcia, and B. J. Soden, "Far-infrared: a frontier in remote sensing of Earth's climate and energy balance," Proc. SPIE **4485**, 150–158, (2002).
2. S. A. Clough, M. J. Iacono, and J.-L. Moncet, "Line-by-line calculations of atmospheric fluxes and cooling rates: application to water vapor," J. Geophys. Res. **97**, 15761–15785, (1992).
3. C. J. Cox, J. Harries, P. Taylor, P. Green, A. Baran, J. Pickering, A. Last, and J. Murray, "Measurement and simulation of mid- and far-infrared spectra in the presence of cirrus," Q. J. R. Meteorol. Soc. **136**, 718–739 (2010).
4. J. Harries, B. Carli, R. Rizzi, C. Serio, M. Mlynczak, L. Palchetti, T. Maestri, H. Brindley, and G. Masiello, "The far-infrared earth," Rev. Geophys. **46**, RG4004, (2008).
5. M. G. Mlynczak, D. G. Johnson, H. Latvakoski, K. Jucks, M. Watson, D. P. Kratz, G. Bingham, W. A. Traub, S. J. Wellard, C. R. Hyde, and W. Liu, "First light from the far-infrared spectroscopy of the troposphere (FIRST) instrument," Geophys. Res. Lett. **33**, L07704, (2006).
6. D. D. Turner, E. J. Mlawer, G. Bianchini, M. P. Cadeddu, S. Crewell, J. S. Delamere, R. O. Knuteson, G. Maschwitz, M. Mlynczak, S. Paine, L. Palchetti, and D. C. Tobin, "Ground-based high spectral resolution observations of the entire terrestrial spectrum under extremely dry conditions," Geophys. Res. Lett. **39**, L10801, (2012).
7. G. E. Bingham, H. M. Latvakoski, S. J. Wellard, M. G. Mlynczak, D. G. Johnson, W. A. Traub, and K. W. Jucks, "Far-infrared spectroscopy of the troposphere (FIRST): sensor development and performance drivers," Proc. SPIE **5157**, 143–153, (2003).
8. H. Latvakoski and M. Watson, "Performance of highly emissivity 10 to 100 μm blackbodies," presented at 2005 CALCON Technical Conference, Logan, Utah, 22–25 August 2005.
9. H. Latvakoski, M. Watson, S. Topham, D. Scott, M. Wojcik, and G. Bingham, "A high-accuracy blackbody for CLARREO," Proc. SPIE **7808**, 78080X (2010).
10. J. P. Rice and B. C. Johnson, "The NIST EOS thermal-infrared transfer radiometer," Metrologia **35**, 505 (1998).
11. R. U. Datla, J. Neira, T. Ohno, J. P. Rice, H. Latvakoski, K. Slack, J. Borelli, M. Slattery, and J. Lawrence, "NIST thermal-infrared transfer radiometer (TXR) deployments to measure the emissivity and radiance of the LWIRCS and GOES-R ECT blackbodies," presented at 2011 CALCON Technical Conference in Logan, Utah, 29 August–1 September 2011.